Chapter 6

Native Purification and Labeling of RNA for Single Molecule Fluorescence Studies

Arlie J. Rinaldi, Krishna C. Suddala, and Nils G. Walter

Abstract

The recent discovery that non-coding RNAs are considerably more abundant and serve a much wider range of critical cellular functions than recognized over previous decades of research into molecular biology has sparked a renewed interest in the study of structure–function relationships of RNA. To perform their functions in the cell, RNAs must dominantly adopt their native conformations, avoiding deep, non-productive kinetic traps that may exist along a frustrated (rugged) folding free energy landscape. Intracellularly, RNAs are synthesized by RNA polymerase and fold co-transcriptionally starting from the 5′ end, sometimes with the aid of protein chaperones. By contrast, in the laboratory RNAs are commonly generated by in vitro transcription or chemical synthesis, followed by purification in a manner that includes the use of high concentrations of urea, heat and UV light (for detection), resulting in the denaturation and subsequent refolding of the entire RNA. Recent studies into the nature of heterogeneous RNA populations resulting from this process have underscored the need for non-denaturing (native) purification methods that maintain the co-transcriptional fold of an RNA. Here, we present protocols for the native purification of an RNA after its in vitro transcription and for fluorophore and biotin labeling methods designed to preserve its native conformation for use in single molecule fluorescence resonance energy transfer (smFRET) inquiries into its structure and function. Finally, we present methods for taking smFRET data and for analyzing them, as well as a description of plausible overall preparation schemes for the plethora of non-coding RNAs.

Key words RNA folding, Non-denaturing purification, Single molecule fluorescence resonance energy transfer, Non-denaturing RNA transcription, Fluorophore labeling of RNA, Biotin labeling of RNA

1 Introduction

Over the last decade, the classical role of RNA as the messenger between DNA and protein, the legislative and executive branches of molecular biology, has been greatly expanded with the discovery of a multitude of non-protein coding (or non-coding) RNAs [1]. These RNAs have been shown to play a central role in a variety of cellular processes including the regulation of gene expression [2, 3], splicing [4], translation [5] and maintenance of chromosome ends [6].

Frank J. Schmidt (ed.), *RNA-RNA Interactions: Methods and Protocols*, Methods in Molecular Biology, vol. 1240, DOI 10.1007/978-1-4939-1896-6_6,

Furthermore, it has been shown that the effect of secondary structure inherent to the untranslated regions (UTRs) of messenger RNAs (mRNAs) on gene expression has been largely underestimated [7]. As a result, much renewed interest has shifted toward studies of structure and function of RNAs. For example, the discovery of riboswitches has added a new dimension to the role of RNA structure in gene regulation. Riboswitches are structural elements found most commonly in the 5′ untranslated regions (UTRs) of bacterial mRNAs that respond to an intracellular metabolite signal [8]. Binding of this metabolite to a highly conserved aptamer domain induces a structural change in the downstream expression platform. The molecular communication between the aptamer domain and expression platform results in a genetic "off" (or sometimes "on") signal, in which expression of the downstream gene is downregulated, usually through attenuation of transcription or inhibition of translation initiation. A plethora of studies focused on the conformational disparity between the ligand-bound and ligand-free states [9–14] are beginning to yield a detailed picture of the mechanisms by which riboswitches can regulate gene expression. However, the question of how a ligand binding event can cause a downstream conformational change remains largely shrouded. To better understand the complex function of RNA secondary and tertiary structure motifs in gene regulation, as exemplified by riboswitches, it is of great importance to study the conformational changes and folding dynamics inherent in non-coding RNAs.

Ideally, RNA folding and function would be investigated in vivo; however, due to the complexity of the cellular environment and our limited ability to manipulate it, it has become accepted practice to study RNA structure and folding in vitro. Typically, the RNA required to perform these studies is produced either by chemical synthesis or by run-off transcription in vitro from a linearized DNA template using T7 RNA polymerase [15]. Following synthesis or transcription, the most common means of RNA purification is through the use of denaturing polyacrylamide gel electrophoresis (PAGE), followed by gel elution and refolding. This method relies heavily on the assumption that in vitro synthesized RNA will refold into its native and functional structure, and therefore, will give proper insight into its properties in vivo. However, this process requires a variety of harsh denaturants including urea and heat, as well as the exposure to UV light (for detection). In contrast, RNAs generated in vivo fold in the crowded environment of the cell on their own co-transcriptionally and segmentally beginning from the 5′ end [16], or with the aid of a multitude of protein chaperones that aid in navigating an often complex folding-free energy landscape [7, 17, 18]. Recently, an array of studies has shown that the commonly accepted methods of denaturing RNA purification can result in severe conformational heterogeneity where populations of active (properly folded) and

inactive (misfolded) RNA species coexist [19–21], highlighting the need for suitable non-denaturing (native) RNA purification techniques. Such techniques better preserve the co-transcriptional fold of an RNA and thus have the potential to simplify the complexity of an RNA population for further study. This feature is of particular importance for riboswitches that are thought to often switch in a co-transcriptional fashion. However, the challenge then becomes how to attach detectable labels to the RNA as needed for many biophysical in vitro studies.

The purpose of this chapter is to highlight how native RNA purification may be coupled with the attachment of labels that enable single molecule fluorescence resonance energy transfer (smFRET) measurements in particular and label-dependent biophysical studies in general while maintaining the RNA's co-transcriptional fold. smFRET is a highly sensitive technique that can reveal even subtle conformational and dynamic changes in single RNA molecules, thus often capturing transient and/or rare events that are averaged out in more conventional ensemble (bulk) experiments [22–24]. Recently, the capabilities of smFRET have been widely established on a variety of non-coding RNAs, such as ribozymes [25–33], riboswitches [34–36], spliced pre-mRNAs [37] and telomerase RNA [38, 39], underpinning its usefulness in the study of RNA (un)folding by directly measuring unperturbed kinetic rate constants at equilibrium. A particular challenge of such smFRET studies is the need to site-specifically attach both a biotin molecule for surface immobilization (required for extended observation) and a pair of fluorophores for FRET, requiring three orthogonal labeling strategies. In addition to native purification and smFRET measurement techniques, we therefore provide here a selection of proven protocols and examples for the labeling of in vitro transcribed RNAs for smFRET measurements of co-transcriptionally folded samples. We anticipate that combining these protocols in various ways will become increasingly important for studying folding and function of an ever-expanding non-coding RNA universe.

1.1 Combining Native Purification with Labeling of RNA: Overview of Methods

Native purification methods can offer a solution to the formation of heterogeneous RNA populations by avoiding the need for harsh denaturants. Different strategies are used to natively purify RNA that can be broadly classified into two categories. The first set of methods isolates the full-length transcript utilizing either a protein [40–43] or a complementary oligonucleotide [20, 44] that specifically binds an incorporated affinity tag in the RNA, followed by ribozyme or DNAzyme-mediated cleavage to obtain the correct length product. Alternatively, RNA is primed during in vitro transcription with a photocleavable, biotinylated GMP tag that is removed subsequent to affinity purification [45]. A second set of methods directly purifies the RNA from the transcription reaction

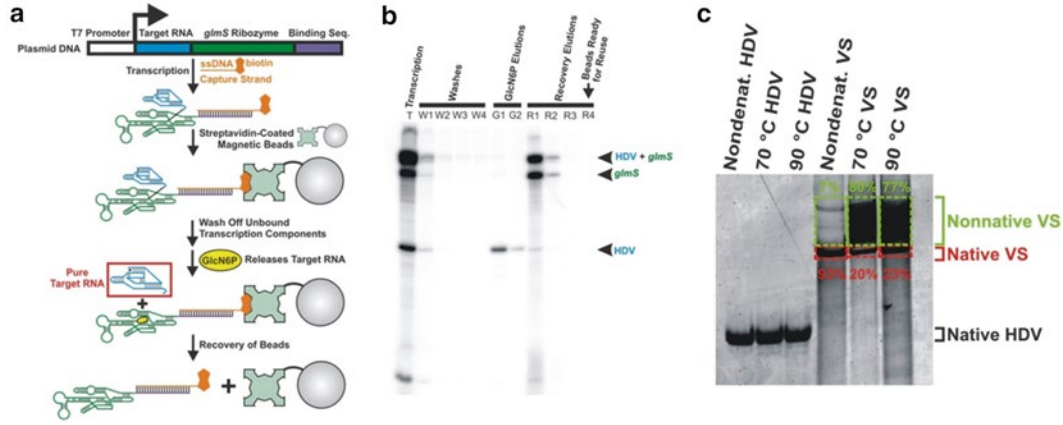

Fig. 1 Native purification of RNA, adapted from ref. 20. Panel (**a**): The purification scheme begins with T7 RNA polymerase transcription of a conjugated RNA composed of target RNA-*glmS* ribozyme-binding sequence. The binding sequence binds to a biotinylated capture strand included in the transcription reaction, and is subsequently incubated with streptavidin-coated beads. Following cleavage by addition of glucosamine-6-phosphate (GlcN6P), the RNA of interest is eluted from the beads without any harsh denaturing steps. Panel (**b**): Representative denaturing PAGE gel showing that the hepatitis delta virus (HDV) ribozyme elutes cleanly from the beads after *glmS*-mediated cleavage. Panel (**c**): Non-denaturing PAGE gel showing that the homogeneously folded VS ribozyme obtained from non-denaturing purification redistributes into multiple bands when heat denatured and refolded

mix using HPLC or a combination of weak anion exchange and size exclusion chromatographies [46, 47]. Although the affinity-based methods generally require more steps and construction of an altered DNA template, they more easily generate the correct length product with precise, homogeneous 5′ and/or 3′ end.

We have developed a simple and rapid RNA native purification technique that uses streptavidin-coated magnetic beads and *glmS* ribozyme-mediated cleavage to generate homogeneous RNA in a short time [20] (Fig. 1). It removes the requirement for large quantities of protein and expensive FPLC systems associated with an earlier version of protein-based affinity purification [41]. The DNA template (Fig. 1a) encodes a full length transcript containing the RNA of interest at the 5′ end, followed by a *glmS* ribozyme sequence and a 3′ binding sequence that is complementary to a 30-nt biotinylated DNA oligonucleotide (capture strand). The in vitro transcription reaction is performed in the presence of the capture strand and, after a phenol–chloroform extraction to remove protein, streptavidin-coated magnetic beads are used to affinity-purify the full length transcript via the hybridized biotinylated capture strand. Any terminated or shorter transcripts and free NTPs are washed away after this binding step. Addition of glucosamine-6-phosphate (GlcN6P) containing buffer to the bead-bound RNA activates the *glmS* ribozyme, resulting in its self-cleavage and

release of the RNA segment of interest (Fig. 1a). The magnetic beads can be easily regenerated by heating to disrupt the biotin–streptavidin interaction and be reused for multiple rounds of purification with little decrease in overall yield. Using this method, sufficient quantities of conformationally homogeneous RNA can be made (Figs. 1b, c), which can be labeled for smFRET studies.

Studying RNA folding and dynamics using smFRET by total internal reflection microscopy (TIRFM) methods requires labeling with donor and acceptor fluorophores and biotin for surface immobilization to increase the time of observation [22, 24]. Although different chemical and enzymatic methods are available for labeling RNA at the 5′ or 3′ end [48], not all of them are compatible with native purification as they involve harsh conditions that could denature the RNA. Here we describe some of the labeling methods that may be used to generate a triply labeled, co-transcriptionally folded RNA sample. Labeling of the 5′ end of RNA can be accomplished by reacting the phosphate group with the carbodiimide cross-linker EDC (1-ethyl-3-[3-dimethylaminopropyl]carbodiimide hydrochloride) and imidazole [49], generating a reactive phosphorylimidazolide group that can be coupled to any primary amine containing molecule such as biotin hydrazide. Alternatively, fluorophore labeling is achieved by reacting the phosphorylimidazolide group with ethylenediamine to generate a free primary amine that can be coupled to any NHS ester-modified molecule [50, 51]. Other methods are available to directly generate RNA with 5′ reactive groups or labels through in vitro transcription with T7 RNA polymerase, since the enzyme can incorporate modifications at the 5′ end of the transcript [52–54]. Periodate chemistry oxidizes the ribose 2′,3′-diol in RNA to aldehyde groups that are reactive with a hydrazide-modified fluorophore or biotin to generate 3′ end-labeled RNA [49]. In addition, enzymatic labeling of the RNA 3′ end can be achieved using T4 RNA ligase [55] or poly(A) polymerase [56]. Poly(A) polymerase is generally used for polyadenylation of RNAs but can also be used to incorporate azide(N_3)-modified NTPs at the 3′ end of RNA [56]. Under optimized conditions, yeast and *E. coli* poly(A) polymerases add a single 2′-N_3-2′-dNTP that can be reacted with an alkyl-derivative of any fluorophore label using "click" chemistry. However, since it is hard to control the number of added nucleotides, 3′-N_3-2′,3′-ddNTPs can be used to incorporate just a single nucleotide at the 3′ end of RNA [56]. Both copper-catalyzed and copper-free "click" chemistry can then be used for labeling [56], but the presence of copper in the reaction leads to degradation of RNA and could alter its native conformation. Recent studies have focused on optimizing solvent conditions for copper-catalyzed click chemistry for labeling RNA to obtain maximum yield with minimal degradation [54, 57]. However, whether these methods preserve the native fold of RNA still needs to be tested. Strain promoted azide-alkyne

cycloaddition (SPAAC) or copper-free click chemistry is a mild and potentially more efficient way of labeling azide-modified RNA with fluorophore-conjugated cyclooctynes. Since the reaction does not require metal ions and also occurs at low temperatures, it is compatible with native labeling of RNA. A variety of fluorophores conjugated to different cyclooctynes are now commercially available for labeling using SPAAC (Clickchemistrytools.com).

In addition to end labeling, in many cases RNA needs to be labeled with one of the fluorophores internally at a specific site for smFRET studies to be most sensitive to a particular conformational change. Site-specific internal labeling of RNA is difficult to accomplish. One relatively easy way is to use fluorophore-labeled short DNA or RNA oligonucleotides that are complementary to a single-stranded region in RNA. This method has been used to study large RNAs and RNA–protein complexes such as RNase P, the group II intron, the ribosome and the spliceosome [26, 37, 58, 59]. In such cases, evolutionarily less conserved and functionally less relevant hairpin loops are extended to facilitate binding of the labeled oligonucleotides. A more commonly used method for internal labeling of smaller RNAs is to end label one of two fragments (the 3′ end of the upstream fragment or the 5′ end of the downstream fragment) and ligate them together so that one of the end labels becomes an internal label [60]. The fragments are individually transcribed and need to fold into the same conformation as adopted in the full length RNA. Some studies have used this strategy to label RNAs for smFRET studies and showed it to work for a two-step ligation with three fragments [61]. DNA or RNA splints are commonly used to bring together two or more RNA fragments for efficient ligation. Among the available ligases, T4 RNA ligase 2 (T4 Rnl-2) is the most efficient enzyme that ligates nicks in double-stranded RNA and works equally well with both DNA and RNA splints [62]. Truncated versions of T4 Rnl-2 are also available that generate less by-products, but require a pre-adenylated substrate [62]. The most important step in generating natively purified and internally labeled RNA is to make sure that the individual RNA fragments used for ligation do not fold into alternative structures. RNA structure probing should be performed on them or secondary structure prediction programs such as MFold [63] may be used to check whether the fragments are likely to fold into any undesired alternate conformations.

1.2 smFRET Measurement and Analysis: General Considerations

Within the last 20 years, the development of single molecule microscopy has revolutionized the field of biosciences [23, 64]. Classically, questions regarding complex biological systems were investigated using bulk ensemble assays that average out rare but often significant idiosyncrasies within a given population of molecules. By contrast, single molecule experiments have the unique capability of revealing the diversity that exists from molecule to

molecule. Observation of one molecule for an extended period of time and/or of many single molecules for limited periods of time will yield information related to that of the entire population as in a bulk ensemble experiment. However, single molecule observation will additionally access the interconversion kinetics of different species at equilibrium as well as reveal transient species, both features difficult to detect otherwise. Moreover, single molecule experiments are advantageous due to their use of very small quantities of sample, eliminating the multimerization effects that bulk experiments may suffer [64]. To this end, a variety of techniques have been developed utilizing the single molecule regime, including single molecule fluorescence microscopy [65, 66], super-resolution imaging and super-accuracy co-localization techniques [67–70], and force microscopy [71–73]. The vast array of applications available today equips scientists with the ability to obtain mechanistic information regarding biological systems that was not possible only a few years ago.

In this chapter, we describe total internal reflection fluorescence (TIRF)-based smFRET microscopy. smFRET has been applied to study the folding of many biologically relevant molecules [22, 74], including RNA [24–39, 75, 76]. It constitutes a non-radiative energy transfer process in which a single dye molecule is excited by a laser. The distance between this "donor" fluorophore and a second "acceptor" fluorophore is reported in real-time through transfer of excitation energy to the acceptor based on an overlap of the donor emission with the acceptor excitation spectrum. As such, the smaller the donor–acceptor distance, the lower (more quenched) the emission of the donor dye and the greater the emission of the acceptor dye. FRET is generally quantified as a FRET efficiency (E), which is given by the Förster equation, $E = \left(1 + \left(\frac{R}{R_0}\right)^6\right)^{-1}$, where R_0 is the Förster radius (or distance) for the specified donor–acceptor dye pair at which their FRET efficiency is 50 %, and R is the donor–acceptor distance. Since every donor and acceptor dye pair has its own specific Förster radius, based on the given overlap of their spectra and the assumption of isotropic relative spatial orientation of their transition dipole moments, they must be chosen carefully and in a manner that will report on the specific distance to be studied. Conversely, the molecule of interest must be labeled in such a way that the distance between the fluorophores is within ~2-fold of their Förster radius, differences in smFRET efficiency are expected between conformational states of interest, and the biological function of the RNA is retained. The process of choosing appropriate labeling sites in an RNA is ameliorated when a crystal or NMR structure is available and hypotheses exist on conformational changes of interest. If no such information is available, chemical probing methods under

varying conditions may reveal residues that are accessible to solvent as suitable for labeling, as well as changes in base-pairing and tertiary interactions that lead to hypotheses on biologically relevant shape changes amenable to smFRET probing.

smFRET in general requires doubly fluorophore-labeled RNA molecules. In addition, for TIRF-based smFRET, RNA molecules must additionally be tethered to the surface of a quartz slide, usually through a streptavidin–biotin interaction, leading to the overall requirement of three RNA modifications. TIRF microscopy utilizes an evanescent field created by the total internal reflection of a laser beam at the quartz–water interface of the slide surface [22]. This results in illumination only of molecules that are directly tethered to the slide surface, as the field penetrates only ~100 nm into the solution, thus reducing background signal. This method of reducing the illuminated volume is advantageous to others, such as diffusion smFRET in which the molecules are freely diffusing through a focused laser beam [24], as TIRF-based smFRET allows for the detection of molecules for extended periods of time and is not limited by the time a molecule spends in a confocal volume. Instead, TIRF-based smFRET observation is limited by the longevity of the fluorophores before they photobleach, which can be extended by the addition of an oxygen scavenging system. We have had particular success with the protocatechuic acid/protocatechuate-3,4-dioxygenase system [77] supplemented with Trolox to decrease photoblinking of the acceptor dye [78], even in complex reaction mixtures [37]. Taken together, this TIRF-based smFRET approach allows for the detection of hundreds of single molecules in one field of view for several tens of seconds at a time. From these data, FRET efficiency histograms are constructed to reveal conformational states, as well as the dwell times before interconversion of states (see smFRET Data Processing Section and [79]).

2 Materials

Make all buffers using autoclaved double-deionized water and store at room temperature unless otherwise specified. Exercise caution to avoid RNase contamination by using Latex gloves at all times and dispose of chemical waste following regulations.

2.1 In Vitro Transcription Using T7 RNA Polymerase

1. 100 μg plasmid DNA coding for the RNA of interest followed by a cassette comprising the *glmS* ribozyme and biotin capture strand (*see* **Note 1**, Fig. 1a and ref. 20 for details). To obtain only the RNA including the cassette, the plasmid must be linearized downstream of the cassette with the appropriate restriction endonuclease (following manufacturer's instructions) prior to the transcription reaction. Once linearized, the

plasmid DNA is extracted with a phenol:chloroform:isoamyl alcohol mix (25:24:1 v/v), ethanol precipitated and resuspended in double-deionized water. Store linearized plasmid at −20 °C.

2. Transcription buffer (10×): 400 mM HEPES-KOH (pH 8.0), 2 M NaCl, 250 mM $MgCl_2$, 50 mM DTT, stored at −20 °C.
3. 5′ biotinylated DNA capture strand complementary to the binding sequence encoded in the plasmid (*see* Fig. 1a). Biotinylation can be performed in house or during synthesis.
4. 100 mM ATP, stored at −20 °C (*see* **Note 2**).
5. 100 mM UTP, stored at −20 °C (*see* **Note 2**).
6. 100 mM CTP, stored at −20 °C (*see* **Note 2**).
7. 100 mM GTP, stored at −20 °C (*see* **Note 2**).
8. T7 RNA polymerase, stored at −20 °C (*see* **Note 3**).
9. Inorganic pyrophosphatase (100 U/mL, New England Biolabs), stored at −20 °C.

2.2 Native Purification of RNA

1. In vitro transcription reaction.
2. Streptavidin-coated magnetic beads (Dynabeads MyOne Streptavidin C1, 1 μm diameter, Invitrogen). Stored at 4 °C.
3. Magnetic particle collector (MPC, DynaMag-2 Magnet, Invitrogen). This MPC can handle 16 standard 1.5–2 mL micro-centrifuge tubes. Larger MPCs are also available that can handle tubes with volumes up to 50 mL, stored at 4 °C.
4. 5 M NaCl in double-deionized water.
5. Glucosamine-6-Phosphate (GlcN6P) stock (≥98 % pure, Sigma-Aldrich). Store at −20 °C.
6. Wash buffer (WB, 1×): 40 mM HEPES-KOH (pH 7.4), 1 M NaCl.
7. Cleavage buffer (CB, 1×): 40 mM HEPES-KOH (pH 7.4), 1 M NaCl, 10 mM $MgCl_2$, 200 μM GlcN6P.
8. Elution buffer (EB, 1×): 10 mM Tris–HCl (pH 8.0).
9. Phenol/chloroform/isoamyl alcohol (25:24:1 v/v, pH 5.2, Fisher Scientific).
10. Chloroform saturated in TE buffer (10 mM Tris–HCl, pH 6.0, 1 mM EDTA).
11. SYBR Gold nucleic acid stain (Invitrogen), stored at −20 °C protected from light.
12. TBE buffer (1×): 89 mM Tris-Borate, 2 mM EDTA (*see* **Note 4**).
13. Typhoon Imager (GE Healthcare).
14. Imaging Software (ImageQuant or ImageJ).

2.3 Biotinylation of the 5′ End of RNA

1. 10 μg in vitro transcribed, natively purified RNA, unlabeled on the 5′ end.
2. Antarctic phosphatase buffer (10×): 500 mM Bis-Tris-Propane-HCl (pH 6.0), 10 mM $MgCl_2$, 1 mM $ZnCl_2$, stored at −20 °C (New England Biolabs).
3. T4 DNA ligase buffer (10×): 500 mM Tris–HCl (pH 7.5), 100 mM $MgCl_2$, 10 mM ATP, 100 mM dithiothreitol (DTT), stored at −20 °C (New England Biolabs).
4. Phenol/chloroform/isoamyl alcohol (25:24:1 v/v, pH 5.2, Fisher Scientific).
5. Chloroform saturated in TE buffer (10 mM Tris–HCl, pH 6.0, 1 mM EDTA).
6. Non-denatured EtOH (>99.5 % pure, Acros), stored at −20 °C.
7. 3 M NaOAc, pH 5.2.
8. 70 % (v/v) EtOH in dH_2O, stored at −20 °C (*see* **Note 5**).
9. EDC reaction buffer (2×): 20 mM K-phosphate (pH 7.0), 300 mM NaCl, 20 mM EDTA.
10. Double-deionized water.
11. 12.5 mg 1-ethyl-3-(3-dimethylaminopropyl)carbodiimide (EDC, Piercenet), stored at −20 °C and kept from moisture.
12. 44 mg biotin hydrazide (Sigma B7639), stored at 4 °C.
13. 0.1 M imidazole (pH 6.0).
14. Illustra NAP-5 column (GE Healthcare).
15. T4 polynucleotide kinase (10 U/μL, New England Biolabs), stored at −20 °C.
16. Antarctic phosphatase (5 U/μL, New England Biolabs), stored at −20 °C.
17. Refrigerated centrifuge (4 °C) with rotor for 1.5 mL tubes (Eppendorf).
18. Vacufuge vacuum concentrator (Eppendorf, optional).

2.4 Fluorophore Labeling 5′ End of RNA with NHS Ester

1. 10 μg in vitro transcribed, natively purified RNA, unlabeled on the 5′ end.
2. Antarctic phosphatase buffer (10×): 500 mM Bis–Tris–Propane–HCl (pH 6.0), 10 mM $MgCl_2$, 1 mM $ZnCl_2$, stored at −20 °C (New England Biolabs).
3. T4 DNA ligase buffer (10×): 500 mM Tris–HCl (pH 7.5), 100 mM $MgCl_2$, 10 mM ATP, 100 mM dithiothreitol (DTT), stored at −20 °C (New England Biolabs).
4. Phenol/chloroform/isoamyl alcohol (25:24:1 v/v, pH 5.2, Fisher Scientific).
5. Chloroform saturated in TE buffer (pH 6.0).
6. Non-denatured EtOH (>99.5 % pure, Acros) stored at −20 °C.

7. 3 M NaOAc, pH 5.2.
8. 70 % (v/v) EtOH, stored at –20 °C (*see* **Note 5**).
9. EDC reaction buffer (2×): 20 mM K-phosphate (pH 7.0), 300 mM NaCl, 20 mM EDTA.
10. Double-deionized water.
11. 12.5 mg 1-ethyl-3-(3-dimethylaminopropyl)carbodiimide (EDC, Piercenet), stored at –20 °C and kept from moisture.
12. 0.1 M imidazole (pH 6.0).
13. Illustra NAP-5 column (GE Healthcare).
14. Ethylenediamine (Piercenet).
15. 0.1 M sodium carbonate buffer (pH 8.7), stored at –20 °C.
16. DMSO (Sigma-Aldrich).
17. NHS-ester derivative of the desired fluorophore, such as Cy3 Mono-Reactive Dye Pack (GE Healthcare), stored at 4 °C (*see* **Note 6**).
18. T4 polynucleotide kinase (10 U/mL, New England Biolabs), stored at –20 °C.
19. Antarctic phosphatase (5 U/mL, New England Biolabs), stored at –20 °C.
20. Refrigerated centrifuge (4 °C) with rotor for 1.5 mL tubes.
21. Vacufuge vacuum concentrator (Eppendorf, optional).

2.5 3′ End Labeling Using Periodate Chemistry

1. 2 nmol in vitro transcribed, natively purified RNA, unlabeled on the 3′ end.
2. 400 mM $NaIO_4$.
3. 3 M NaOAc, pH 5.2.
4. Non-denatured EtOH (>99.5 % pure, Acros), stored at –20 °C.
5. 70 % (v/v) EtOH, stored at –20 °C (*see* **Note 5**).
6. Hydrazide derivative of the desired fluorophore, such as Alexa Fluor 488 Hydrazide (Invitrogen), stored at 4 °C (*see* **Note 6**).
7. Illustra NAP-5 column (GE Healthcare).
8. Double-deionized water.
9. Refrigerated centrifuge (4 °C) with rotor for 1.5 mL tubes (Eppendorf).
10. Vacufuge vacuum concentrator (Eppendorf, or other vendor, optional).

2.6 3′ End Labeling Using Poly(A) Polymerase and "Click" Chemistry

1. Yeast poly(A) polymerase (600 U/μL, Affymetrix), stored at –20 °C.
2. Yeast poly(A) polymerase (PAP) reaction buffer (5×): 500 mM Tris–HCl (pH 7.0), 400 mM KCl, 3 mM $MnCl_2$, 0.1 mM EDTA, 1 mM DTT, 500 μg/mL acetylated BSA, 50 % (v/v) glycerol (Affymetrix), stored at –20 °C.

3. *E. coli* poly(A) polymerase (5 U/μL, New England Biolabs), stored at −20 °C (*see* **Note 7**).
4. *E. coli* poly(A) polymerase reaction buffer (10×): 500 mM Tris–HCl (pH 7.9), 2.5 M NaCl, 100 mM $MgCl_2$ (New England Biolabs), stored at −20 °C.
5. 10 mM ATP (New England Biolabs), stored at −20 °C.
6. 50 mM phosphate buffer (pH 7.0) at 25 °C, 0.1 M KCl, 1 mM Mg^{2+}.
7. 1 μmol 3′-N_3-2′,3′-ddATP (Trilink Biotechnologies).
8. DBCO (Dibenzylcyclooctyne) containing fluorophores, such as DBCO-Fluor 488 (Jena Biosciences), stored at −20 °C (*see* **Note 6**).
9. Phenol/chloroform/isoamyl alcohol (25:24:1 v/v, pH 5.2, Fisher Scientific).
10. Illustra NAP-5 column (GE Healthcare).
11. 3 M NaOAc, pH 5.2.
12. Non-denatured EtOH (>99.5 % pure, Acros), stored at −20 °C.
13. 70 % (v/v) EtOH, stored at −20 °C (*see* **Note 5**).
14. Refrigerated centrifuge (4 °C) with rotor for 1.5 mL tubes (Eppendorf).
15. Vacufuge vacuum concentrator (Eppendorf, or other vendor, optional).

2.7 Internal Labeling of Large RNA Using Short Fluorophore Labeled Oligonucleotides

1. DNA oligonucleotides (14–16 bases long) with 5′ or 3′ amino modification complementary to unstructured regions of the RNA of interest (*see* **Note 8**).
2. NHS-ester derivative of the desired fluorophore, such as Cy3 Mono-Reactive Dye Pack (GE Healthcare), stored at 4 °C (*see* **Note 5**).
3. Hybridization buffer: 50 mM Tris–HCl (pH 7.5), 100 mM KCl, 1 mM $MgCl_2$ (*see* **Note 9**).

2.8 RNA Ligation

1. T4 RNA ligase 2 (T4 Rnl-2, 10 U/μL, New England Biolabs), stored at −20 °C.
2. T4 RNA ligase 2 reaction buffer (10×, Rnl-2 buffer): 500 mM Tris–HCl (pH 7.5), 20 mM $MgCl_2$, 10 mM DTT, 4 mM ATP (New England Biolabs), stored at −20 °C.
3. DNA splint oligonucleotide, stored at −20 °C (*see* **Note 10**).
4. DNase I (RNase-free, 2 U/μL, New England Biolabs), stored at −20 °C.

2.9 Surface Treatment of Slides

1. Quartz slides (3 in. × 1 in. × 1 mm thick, G. Finkenbeiner Inc.) with holes drilled on either side to allow for input and output flow of material (*see* **Note 11**).

2. Glass coverslips (24 × 30 mm, VWR International).
3. Alconox detergent (Alconox, Inc.).
4. Double-sided tape (1/2 in. wide, ~100 μm thick, 3 M).
5. Polypropylene coplin jars (Fisher Scientific).
6. Sonicator.
7. 70 % (v/v) EtOH.
8. Methanol (Fisher).
9. 1 M KOH (*see* **Note 12**).
10. Hydrogen peroxide, 35 % (w/w) solution in water (Fisher), stored at −20 °C.
11. Ammonium hydroxide, NH_4OH, or 30 % (w/w) solution of NH_3 in water (Fisher), stored at −20 °C.
12. Propane torch.
13. Immunopure biotinylated bovine serum albumin (bBSA) (Fisher), stored at 4 °C (*see* **Note 13**).
14. T50 buffer (1×): 10 mM Tris–HCl (pH 7.0), 50 mM NaCl.
15. Immunopure streptavidin (Invitrogen) (*see* **Note 14**).
16. Aminosilane reagent, APTES (N-(2-aminoethyl)-3-aminopropyltrimethoxysilane, Sigma).
17. Biotin-PEG (MW 5000, Laysan Bio Inc.), stored at −20 °C.
18. Methoxypolyethylene glycol (mPEG succinimidyl valerate, MW 5,000, Laysan Bio Inc.), stored at −20 °C in the dark.
19. PEGylation buffer (1×): 10 mM sodium bicarbonate (pH 8.5) (*see* **Note 15**).
20. PEGylation reaction mix: Dissolve 8 mg biotin-PEG, 80 mg mPEG in 320 μL PEGylation buffer in a microcentrifuge. Mix the solution thoroughly and vortex to dissolve the PEG. Centrifuge the tube at 9,000 × *g* for 1 min to remove bubbles.
21. DST buffer: Prepare fresh by dissolving 10 mg DST (Sulfodisuccinimidyl tartrate) in 350 μL PEGylation buffer. Prepare this solution immediately before use.
22. N_2 gas.
23. smFRET buffer (1×): 50 mM Tris–HCl (pH 7.5), 100 mM KCl, 1 mM $MgCl_2$.
24. OSS buffer (1×): 50 mM Tris–HCl (pH 7.5), 100 mM KCl, 1 mM $MgCl_2$, 5 mM protocatechuic acid (PCA), 50 nM protocatechuate-3,4-dioxygenase (PCD), 2 mM Trolox (*see* **Note 16**).

3 Methods

The following methods are used for native purification of RNA and labeling with an aim to preserve its co-transcriptionally folded conformation. At each step, care should be taken to maintain physiologically relevant conditions (pH 5–8, 10–100 mM monovalent cations and/or 1–10 mM Mg^{2+}) to prevent denaturation of RNA and preserve its tertiary structure. In addition, use of high laser intensity in smFRET experiments may lead to photodamage to RNA and therefore, the signal-to-noise ratio should be optimized at the lowest laser power possible.

3.1 In Vitro Transcription Using T7 RNA Polymerase

The following protocol is intended for the transcription of unlabeled RNA molecules for the study of RNA folding by smFRET.

1. This protocol for a 2 mL transcription reaction requires the use of 100 μg of linearized plasmid DNA as described in Subheading 2 (*see* **Note 17**).
2. Prepare the following reaction in a conical 15 mL reaction tube. All reactants should be thawed completely and T7 RNA polymerase should be added to the reaction last.

10× Transcription Buffer	200 μL
100 mM ATP	80 μL
100 mM UTP	80 μL
100 mM CTP	80 μL
100 mM GTP	80 μL
5′-Biotinylated capture strand (*see* **Note 18**)	3 μM
Linearized dsDNA Template	50 nM
PP_iase	1.2 U
T7 RNA Polymerase	0.1 mg/mL
Double-deionized H_2O	Adjust to bring final volume to 2 mL

3. Incubate the reaction at 37 °C for 4 h.

3.2 Native Purification of RNA

The following protocol is used to purify in vitro transcribed RNAs in their native conformation. This protocol was developed for the VS ribozyme that folds into a heterogeneous population upon heat annealing but can be applied to any RNA of interest.

1. The presence of protein (RNAP, PP_iase) in the in vitro transcription reaction results in beads sticking to the sides of the microcentrifuge tubes during purification and decreases

the yield of RNA. Remove protein using phenol/chloroform extraction as follows:

(a) Add an equal volume of phenol/chloroform/isoamyl alcohol to the transcription reaction and mix gently by inverting the microcentrifuge tube few times.

(b) Centrifuge the tube at 15,000 × *g* for 2 min.

(c) Pipet the top aqueous layer into a fresh tube. Avoid collecting the protein at the interphase between the aqueous and organic phase.

(d) Centrifuge at 15,000 × *g* for 2 min and collect the top aqueous layer. This removes any residual protein contaminants.

(e) Measure the volume and add equal volume of chloroform to the aqueous layer.

(f) Mix gently by inverting the tube a few times and centrifuge at 15,000 × *g* rpm for 2 min.

(g) Collect the top aqueous layer into a clean microcentrifuge tube.

2. Measure the volume and using 5 M NaCl stock, bring the final concentration of NaCl to 1 M.
3. Pipet 100 µL (1 mg) of streptavidin-coated beads and remove the storage buffer using the MPC (*see* **Note 19**). Wash with beads with WB at least three times and remove the WB.
4. Add the phenol/chloroform extracted transcription reaction to the bead pellet and mix gently with a pipette. Tumble the tube at room temperature for 30 min. This step results in binding of RNA:capture strand complexes to the beads.
5. Remove the supernatant (S) by placing the tube in the MPC (*see* **Note 19**) and wash the beads with WB four times to remove any non-specifically bound RNA. Save the supernatant (S) and the washes (W1–W4) for later analysis using denaturing PAGE.
6. Add 100 µL of CB that contains glucosamine-6-phosphate (GlcN6P) to the bead pellet, mix a few times with a pipette and incubate at room temperature for 2 min (*see* **Note 20**).
7. Collect the supernatant which contains the natively purified RNA. The cleavage step can be repeated to increase the yield slightly.
8. Wash the beads three times with EB and save for later analysis using denaturing PAGE. On the fourth wash with EB, incubate at 70 °C for 5 min and save the supernatant (R1).
9. Wash the beads with EB one more time, incubate at 70 °C for 5 min and collect the supernatant (R2).

10. Wash the beads two times with EB and save the washes (R3–R4). These washes remove the bound RNA and regenerate the beads for more rounds of purification.
11. Place all the collected supernatants on the MPC and remove any residual beads.
12. To 20 μL of each supernatant fraction, add an equal amount of denaturing loading buffer and run a denaturing gel at 20 W for 2 h.
13. Stain the gel in 1:100,000 dilution of SYBR Gold in 1× TBE for 5 min.
14. Image the gel using a Typhoon Imager with an excitation of 488 nm, an emission bandpass of 530 ± 10 nm and a PMT setting of 500 V. Quantification of bands can be accomplished using ImageQuant or ImageJ software.

3.3 Biotinylation of 5′ End of RNA

The following protocol is used to biotinylate unlabeled RNA molecules at the 5′ end for subsequent attachment to a solid surface for TIRF smFRET measurements.

1. In order to obtain a monophosphate at the 5′ end of the RNA for biotin attachment via EDC coupling, prepare the following reaction: 5 μg RNA, 10 μL Antarctic phosphatase buffer, and 5 units Antarctic phosphatase in a volume of 50 μL (*see* **Note 21**).
2. Incubate this reaction for 30 min at 37 °C.
3. Remove the enzyme by a phenol–chloroform extraction as described in **step 1** in Subheading 3.2. If needed, the resulting stock can be stored at −20 °C.
4. For monophosphate addition, prepare the following reaction: 10 μL (1 μg) of dephosphorylated RNA (from above reaction), 5 μL of 10 × T4 DNA Ligase buffer, and 20 U of polynucleotide kinase in a total volume of 50 μL (*see* **Note 21**).
5. Incubate this reaction at 37 °C for 1 h.
6. To remove the enzyme, phenol–chloroform extract the RNA.
7. Precipitate the RNA with EtOH as follows:
   (a) Add 2.5 volumes of non-denaturing EtOH and 1/10 volume of 3 M NaOAc (pH 5.2) to the RNA mixture.
   (b) Incubate the mixture for 30 min at −20 °C.
   (c) Spin the mixture at 4 °C for 30 min in a centrifuge at 15,000 × *g*.
   (d) Discard the supernatant and wash the resulting pellet with 500 μL of cold 70 % (v/v) EtOH.
   (e) Spin the mixture at 4 °C in a centrifuge at 15,000 × *g* for 30 min.
   (f) Discard the supernatant and dry the resulting pellet by incubating at 37 °C for ~10 min, or through the use of a Vacufuge vacuum concentrator.

8. Resuspend the RNA pellet in 37.5 μL 2× EDC reaction buffer and 37.5 μL autoclaved double-deionized water.
9. Add 12.5 mg of EDC to the RNA solution from step 8. Vortex to dissolve and centrifuge to collect contents (*see* **Note 22**).
10. Add 44 mg of biotin hydrazide to 1 mL of autoclaved water. Biotin hydrazide will not completely dissolve. This solution can be stored at −20 °C for future use.
11. To the RNA/EDC solution, add 10 μL of the biotin hydrazide slurry, taking care to mix well before pipetting to ensure sufficient transfer.
12. Add 315 μL of 0.1 M imidazole, pH 6.0 (*see* **Note 23**).
13. Incubate the reaction at room temperature overnight (12–16 h) (*see* **Note 24**).
14. To remove any non-reacted EDC and its byproducts, use a NAP-5 column (*see* **Note 25**).
15. Precipitate the RNA by repeating **step 7**. Resuspend the RNA in dH_2O and store at −20 °C.

3.4 Fluorophore Labeling of 5′ End with NHS Ester

This protocol is intended for the purpose of labeling RNA molecules at the 5′ end via NHS-ester dye.

1. Follow **steps 1–10** exactly as written in Subheading 3.3.
2. Dissolve ethylenediamine to final concentration of 0.25 M in a volume of 100 μL in 0.1 M imidazole, pH 6.0.
3. Add 12.5 mg of EDC to the RNA solution from **step 1**. Vortex to dissolve and centrifuge to gather contents (*see* **Note 22**).
4. Add 50 μL of the ethylenediamine solution to the EDC/RNA solution. Vortex to dissolve and centrifuge to gather contents.
5. Add an additional 200 μL of 0.1 M imidazole, pH 6.0 (*see* **Note 23**).
6. Incubate the reaction at 37 °C for 3 h.
7. To remove any non-reacted EDC and its byproducts, use a NAP-5 column (*see* **Note 25**).
8. Precipitate the RNA with EtOH following **step 7** from Subheading 3.3.
9. Dissolve the resulting pellet in 20 μL of 0.1 M sodium carbonate buffer pH 8.7.
10. Dissolve one dye pack of desired fluorophore, such as Cy3 Mono-Reactive Dye Pack (GE Healthcare) in 30 μL DMSO. Add dissolved Cy3 dye to RNA mix. Wrap in aluminum foil to protect from light (*see* **Note 26**).
11. Tumble reaction mixture at room temperature for 4 h in the dark.

12. Bring total reaction volume up to 0.5 mL with autoclaved H_2O.
13. Desalt RNA and remove unreacted dye using a NAP-5 column (*see* **Note 25**).
14. Precipitate the RNA with EtOH.
15. Resuspend the pellet in autoclaved double-deionized water. Store at −20 °C and keep wrapped in aluminum foil to protect the dye from light.

3.5 RNA 3′ End Labeling with Fluorophore Using Periodate Chemistry

This protocol is intended for fluorophore labeling of natively transcribed RNA at the 3′ end.

1. To oxidize the 2′–3′ diols of the RNA to aldehydes, combine the following reaction: 5 μM RNA, 2.5 μL of 400 mM $NaIO_4$, 13.33 μL of 3 M NaOAc, pH 5.2 in a volume of 400 μL.
2. Incubate the reaction on ice for 50 min.
3. Precipitate the RNA following **step 7** from Subheading 3.3.
4. Dissolve the resulting pellet in 13.33 μL of 3 M NaOAc, pH 5.2 and 1 mM of the hydrazide derivative of the desired fluorophore, such as Alexa Fluor 488 Hydrazide (Invitrogen) in a total volume of 400 μL.
5. Tumble the reaction overnight at 4 °C in the dark.
6. Precipitate the RNA with ethanol.
7. Remove unreacted dye from labeled RNA by using a NAP-5 column (*see* **Note 25**).
8. Precipitate the RNA with ethanol.
9. Resuspend the pellet in double-deionized water. Store at −20 °C and keep wrapped in aluminum foil to protect the dye from light.

3.6 Labeling 3′ End of RNA Using Poly(A) Polymerase and "Click" Chemistry

Use the following protocol to label the 3′ end of RNA with a single 2′-N_3-2′-dNTP.

1. For 3′ end labeling with 2′-N_3-2′-dNTP, where N = C, G, U, dATP is the best substrate, but yeast PAP adds more than one dATP and therefore only C, G, U are used with it; therefore use the following protocol:
   (a) Assemble the reaction in 1× yeast PAP reaction buffer at 5 μM final RNA concentration, 500 μM 2′-N_3-2′-dNTP (N = C, G, U) and 24 U/μL yeast PAP.
   (b) Incubate the reaction at 37 °C for 20 min for 2′-N_3-2′-dCTP, 2 h for 2′-N_3-2′-dGTP or 5 min for 2′-N_3-2′-dUTP. The incubation time may vary for different RNAs and needs to be optimized.

2. For labeling with 2′-N_3-2′-dATP (as the nucleotide substrate that *E. coli* PAP best accepts in 2′-azide modified form), use the following protocol:
   (a) Prepare the following reaction: 0.25 U/μL of *E. coli* PAP in 1× E.coli PAP reaction buffer, 1 mM ATP, 2.5 mM $MnCl_2$.
   (b) Incubate the reaction at 37 °C for 20 min.
   (c) Remove free unincorporated 2′-N_3-2′-dNTPs using a NAP-5 column (*see* **Note 25**).
3. Perform a phenol–chloroform extraction following **step 1** of Subheading 3.2 to remove the enzyme and stop the reaction.
4. Ethanol precipitate the labeled RNA following **step 7** in Subheading 3.3.
5. Label ~1 μM of the 2′-N_3 modified RNA with 50 μM of any DBCO-label (biotin or fluorophore) in 50 mM phosphate buffer (pH 7.0), 0.1 M KCl, 1 mM Mg^{2+} for 2 h at 37 °C.
6. Ethanol precipitate the labeled RNA and resuspend in a suitable buffer (*see* **Note 27**).
7. Labeling efficiency can be checked using a denaturing PAGE gel and, for fluorophore labeling, scanning with a Typhoon scanner.

3.7 Internal Labeling of Large RNA Using Short Fluorophore-Labeled Oligonucleotides

Follow the protocol below to hybridize a short fluorophore-labeled oligonucleotide to unstructured regions in larger RNAs that may not be amenable to the techniques listed above.

1. Label the 3′ amino-labeled oligonucleotide with the Monofunctional NHS ester dye following **steps 9–15** of Subheading 3.4. Use 3–5 nmol of oligonucleotide in 0.1 M sodium bicarbonate buffer.
2. Dissolve the fluorophore-labeled oligonucleotide and the RNA of interest in hybridization buffer at 1:5 molar ratio and incubate at 37 °C for 1 h (*see* **Note 9**).
3. For better hybridization efficiency, use at least 100 nM of the labeled oligonucleotide (*see* **Note 28**).

3.8 RNA Ligation

The following protocol is used for ligating two RNA molecules using a DNA splint (*see* **Note 29**).

1. Aliquot 10–20 pmol of each RNA strand to be ligated in a microcentrifuge tube.
2. Add equimolar concentration of DNA splint oligonucleotide.
3. Incubate the reaction at 37 °C for 30 min in final 1× Rnl-2 buffer concentration. This leads to formation of RNA–DNA hybrid with the 5′ phosphate and 3′ hydroxyl of both RNA strands adjacent to each other, forming a nick.

4. Add 1 U T4 Rnl-2 and incubate the reaction at 37 °C for 30 min.
5. Add $CaCl_2$ to a final concentration of 0.5 mM to the reaction.
6. Add 1 U of DNase I and incubate at 37 °C for 30 min. DNase I will degrade the DNA splint allowing the RNA to fold fully into its native conformation.
7. Remove the protein by phenol–chloroform extraction as described in **step 1** in Subheading 3.2 to stop the reaction.
8. Ligation efficiency can be checked by running a denaturing PAGE gel.

3.9 Slide Preparation Using PEG Coating and bBSA-Streptavidin Coupling

PEG-coated slides are used for single molecule studies on RNA–protein complexes. PEG prevents non-specific binding of proteins to the glass surface.

1. Clean the slides using the following protocol (*see* **Note 30**):
   (a) If slides have been used previously, remove the tape and epoxy resin on the slides by boiling them in water on a hotplate for ~20 min. The epoxy turns yellow when soft and can be scraped off using a razor blade.
   (b) Scrub (*see* **Note 31**) the slides with a thick paste of Alconox and rinse with tap water.
   (c) Sonicate the slides in a 10 % (w/v) Alconox solution for 30 min in polypropyl coplin containers. Rinse the slides thoroughly with double-deionized water.
   (d) Scrub and rinse the slides with methanol/ethanol and rinse with double-deionized water. Optionally, slides can be sonicated in double-deionized water for 10 min.
   (e) Boil the slides in 100 mL double-deionized water, 20 mL NH_4OH, 20 mL 30 % H_2O_2 (5:1:1 v/v) for 30 min. Rinse the slides thoroughly with double-deionized water. This step removes any organic material stuck to the surface and restores silanol groups on the surface. It is optional but helpful in cleaning very dirty slides.
   (f) Sonicate the slides in 1 M KOH in polypropyl containers for 30 min and rinse them with double-deionized water.
   (g) Sonicate the slides in double-deionized water for 10 min.
   (h) Flame the slides using a propane torch slowly spending 1–2 min on each side. Cool the slides by blowing nitrogen over them or let them sit at room temperature for 10 min on clean steel rails while keeping the center of the slides free from contact (*see* **Note 32**).

2. Clean the polypropylene coplin jars using the following protocol:
   (a) Sonicate in 1 M KOH for 20 min.
   (b) Dispose of KOH and rinse thoroughly with double-deionized water.
   (c) Rinse with methanol and sonicate in methanol for 20 min.
   (d) Dispose of methanol, rinse with methanol and dry using N_2 gas.
3. Perform aminosilanization of the slide surface using the following protocol:
   (a) Allow aminosilane to reach room temperature for ~2 h in the dark.
   (b) To 98 mL acetone, add 2 mL of the aminosilane reagent (APTES) in a clean beaker or flask. Approximately 70 mL is required for each reaction container with five slides.
   (c) Pour the aminosilanization mix into the polypropylene coplin jar covering the slides.
   (d) Incubate at room temperature for 10 min.
   (e) Sonicate for 1 min and incubate at room temperature for 10 min.
   (f) Dispose of the reaction mix and rinse thoroughly with double-deionized water.
   (g) Dry the slides with N_2 gas.
4. Perform PEGylation using the following protocol:
   (a) Clean empty pipette tip boxes to hold the slides and place water in the bottom to maintain a humid environment for the PEGylation reaction.
   (b) Take out PEG bottle from the freezer and let it sit at room temperature in dark.
   (c) Place slides in pipette tip boxes and carefully pipette 70 μL of PEG solution onto the middle of the slide.
   (d) Place coverslip carefully over the slide on top of the PEG solution avoiding air bubbles.
   (e) Incubate for 2–3 h (or overnight) at room temperature in dark using the tip boxes.
   (f) Rinse thoroughly with double-deionized water and dry in N_2 gas. Carefully pipette 70 μL of DST buffer onto each slide.
   (g) Place coverslip on top of the slide and DST buffer avoiding air bubbles.
   (h) Incubate at room temperature for 30 min in the dark in the pipette tip boxes.

(i) Rinse thoroughly with double-deionized water and dry in nitrogen.

(j) Assemble the slides according to your requirements.

(k) Store the slides in a dark and dry place. They could be stored in corning tubes covered by black tape or in polypropylene containers under N_2 gas.

To immobilize RNA through biotinylated-BSA coating on the quartz slides, the following protocol can be used. This protocol can be used when proteins will not be used in an smFRET experiment.

1. Clean slides as in **step 1** described previously.
2. Prepare microfluidic channel on the surface of each slide as shown in (ref.) (*see* **Note 33**).
3. Flow 80 μL of biotinylated-BSA through the microfluidic channel. Allow it to bind to the glass surface non-specifically at room temperature for 10 min.
4. Wash unbound bBSA out of the channel with 100 μL of T50 buffer.
5. Flow 80 μL of streptavidin through the microfluidic channel. Allow to equilibrate at room temperature for 5 min.
6. Wash unbound streptavidin out of the channel with 100 μL smFRET buffer.
7. Flow 100 μL of ~20–50 pM biotinylated and fluorophore-labeled RNA through the prepared microfluidic channel. Allow to bind for 5 min in the dark to avoid photobleaching of fluorophores.
8. Check the surface density of the immobilized RNA. If the density of molecules is low, increase the concentration of labeled RNA (*see* **Note 34**).
9. Wash unbound RNA out of the channel with 100 μL of smFRET buffer.
10. Flow 100 μL of OSS buffer through the channel to reduce photobleaching and blinking of the fluorophores. Allow to react in the dark for 5 min (*see* **Note 35**).
11. Record smFRET movies at the required time resolution (generally 10–100 ms). Custom-made programs written in Visual C++, WinView, or ImageJ are normally used for recording smFRET movies.

3.10 Prism-Based TIRF smFRET Data Processing

Following acquisition of the raw data, they must now be processed in such a way that FRET values and kinetic parameters can be extracted [79]. Generally, scripts most commonly written for the programs IDL or MATLAB are used to calculate the FRET data

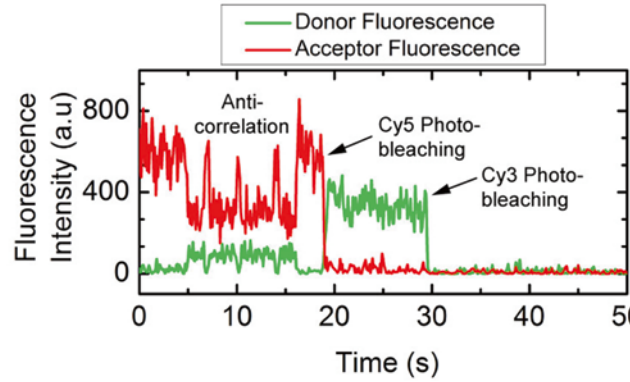

Fig. 2 Characteristics of an smFRET trajectory suitable for analysis. A suitable trace will display two photoactive fluorophores (*dark red*, acceptor; *light green*, donor) that exhibit single-step photobleaching, as well as clear anti-correlation during FRET (Color figure online)

collected from the raw image data. Once the data are accumulated from multiple fields of view and across different channels, individual trajectories must be selected as appropriate for smFRET analysis. Before selecting traces, it is beneficial to establish selection criteria for all trajectories, as this process is often done by eye and can be subject to bias. Single molecules displaying suitable characteristics for smFRET analysis display a variety of characteristics, including, but not limited to (Fig. 2):

- Molecules must have photoactive fluorophores—establish an intensity threshold.
- If applicable, must be doubly labeled—for molecules exhibiting little-to-no FRET, a short excitation of the acceptor fluorophore at the end or intermittently throughout the trajectory can be used to probe for the presence of acceptor dye.
- If FRET is observed, molecules must display clear anticorrelation between the donor and acceptor intensities.
- Single-step photobleaching of each fluorophore toward the end of the trajectory.

After all unsuitable trajectories are discarded, the simplest way to visualize single molecule data is through the creation of FRET population histograms by sampling a small subset of all the available traces in a data set (Fig. 3). For example, FRET values within the first 100 frames of all single molecule trajectories are binned together and plotted as a histogram. When the data are fit with a sum of Gaussian functions, a variety of characteristics inherent in the data set are brought to light, including the mean FRET values sampled by the molecules, as given by the centers of the peaks of each Gaussian distribution. In addition, the relative likelihood of

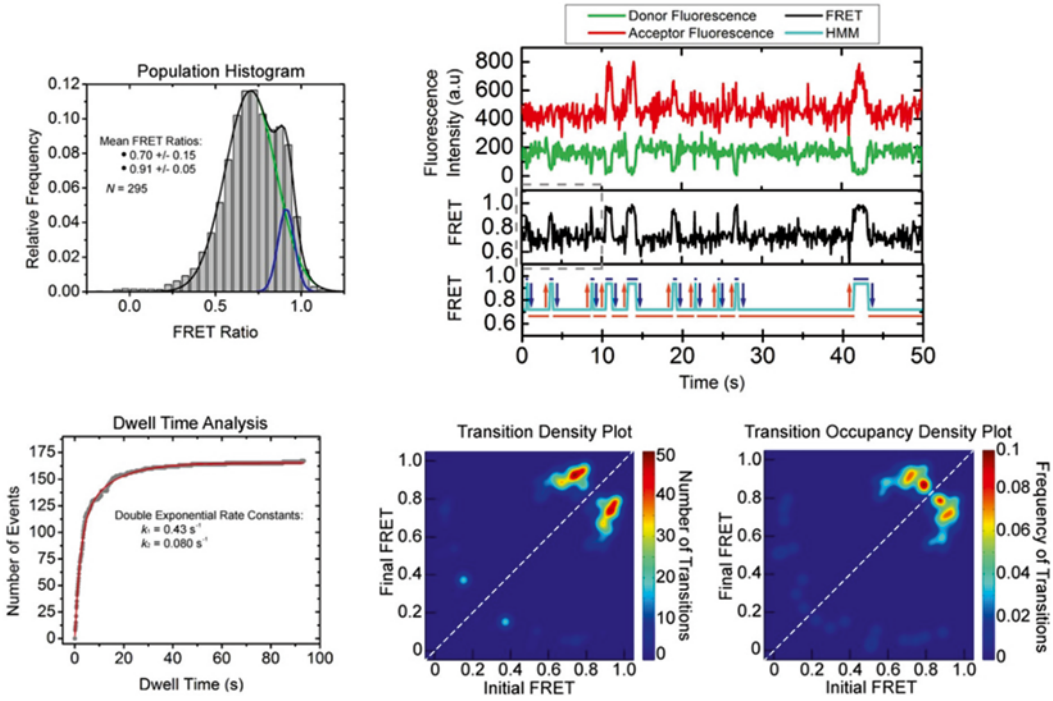

Fig. 3 smFRET data analysis [79]. From a large collection of smFRET traces (*top right panel*), FRET population histograms (*top left panel*) are constructed by binning the first 10 s of FRET data (*grey box* around *black line* in FRET trace). Rate constants describing the interconversion between FRET states are derived from the cumulative dwell times spent in each FRET state (*purple* and *orange lines* in FRET trace). Finally, TDPs and TODPs are created to describe the number of transitions as well as the frequency of transitions between FRET states (*purple* and *orange arrows* in the FRET trace) (Color figure online)

time spent in each state is given by the area under each peak. Finally, the relative widths of each peak can yield insight into underlying ensembles of unresolved conformations. Further analysis is needed to bore out the existence of these states, however.

FRET population histograms are useful for the above reasons; however, they do not reveal any kinetic information for a given data set. To this end, statistical algorithm Hidden Markov Modeling (HMM) has been widely utilized to bore out the FRET states sampled in complex trajectories and the path a molecule takes in order to transition from one state to the next [79, 80]. The most commonly used programs for HMM analysis on smFRET trajectories are HaMMy [80], vbFRET [81], and QuB [82]. All three of these programs are publicly available and can be used to extract the dwell times of molecules in a number of FRET states [79]. By plotting the cumulative population of a data set's dwell times and fitting with a single- or multi-exponential curve, then correcting for the limits imposed by the observation time window and photobleaching [29], one can furthermore obtain the rate constant

for interconversion between two FRET states (Fig. 3). Finally, transition density plots (TDPs) are a useful tool for further visualization of the transitions between FRET states, as they illustrate the frequency of transitions in a three-dimensional heat map (Fig. 3). To remove the bias toward fast, frequently occurring transitions inherent in TDPs, transition occupancy density plots (TODPs) can be used to plot the percentage of molecules displaying a certain transition. For a more in-depth discussion of data processing of single molecule trajectories, we refer to [79].

3.11 An Example: smFRET of the Thermoanaerobacter tengcongensis preQ$_1$ Riboswitch

Here we provide an example of an smFRET study of the translationally operating *Thermoanaerobacter tengcongensis* (*Tte*) preQ$_1$ riboswitch. Binding of the preQ$_1$ ligand by the highly conserved *Tte* aptamer domain in the 5′ UTR of mRNA induces a downstream conformational change in which the Shine-Dalgarno sequence becomes occluded by formation of a pseudoknot, thus inhibiting translation initiation [13, 83]. Our RNA for smFRET probing was designed with the prospect of visualizing loop L3 docking and helix P2 formation as a function of ligand binding; therefore, the RNA was labeled with the donor (DY547) dye on the 3′ end and the acceptor (Cy5) dye in the L2 loop [84]. The riboswitch RNA was immobilized to the quartz slide via a 5′ biotin modification. Donor and acceptor intensities of individual molecules with the appropriate smFRET qualities were collected and representative traces are shown in Fig. 3. FRET population histograms were constructed as a function of ligand concentration, demonstrating two subpopulations consisting of a mid and high FRET conformation (Fig. 3). As ligand concentration is increased, the population of the high FRET state increases at the expense of the mid FRET state, indicating that the high FRET state represents the fully folded, ligand bound conformation seen in the crystal structure [84]. Coarse-grained simulations of corresponding RNA distance distributions confirmed this hypothesis. From the same data set, dwell time analyses can be performed, in which the rate constants of interconversion between the mid and high FRET states at various ligand concentrations are compared. Additionally, these transitions can be visualized by transition density plots (TDPs) and transition occupancy density plots (TODPs) (Fig. 3).

3.12 Envisioned Application of Native Labeling Methods to smFRET of Heterogeneously Folding RNAs

The labeling methods presented in this article were chosen to complement the native co-transcriptional folding maintained by the non-denaturing RNA purification methods developed in our laboratory and others. From these protocols, one can begin with plasmid DNA, which encodes for the RNA of interest, and design various avenues to producing a homogenously folded, triply labeled RNA suitable for smFRET analysis (Fig. 4). For example, it is plausible that small RNAs (<200 nt) with hierarchal tertiary structures can be labeled through the RNA ligation method depicted in

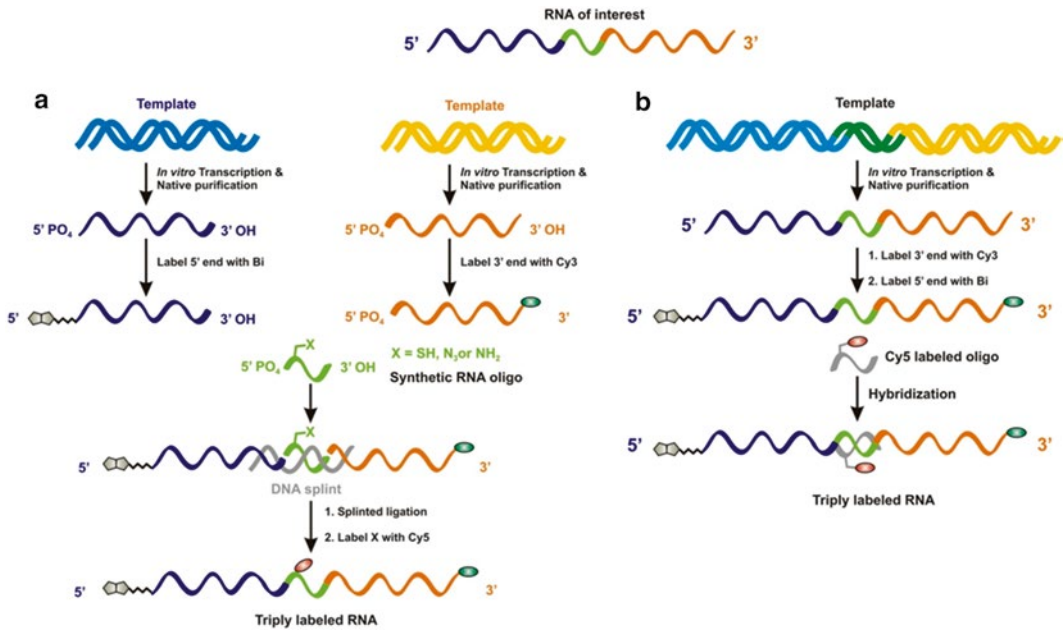

Fig. 4 Creating a triply-labeled RNA for smFRET analysis. Panel (**a**): For shorter RNAs that may exhibit hierarchal folding behavior, the RNA can be segmented into three pieces. The 5′ and 3′ pieces may be transcribed, natively purified and 5′ and 3′ end labeled, whereas the middle piece can be synthetically produced with an amino, sulfhydryl or azide label. Following a two-step splinted ligation, the synthetic modification is used to conjugate a fluorophore using the protocols presented herein. Panel (**b**): For longer RNAs, hybridization of a complementary labeled oligonucleotide is used to create an internal fluorophore (or biotin) label

Fig. 4a. Since RNA structures fold in a hierarchal manner such that secondary structure precedes tertiary structure formation, it is expected that for many RNAs 5′ and 3′ segments can be transcribed separately from one another. These shorter RNA fragments can be modified using the protocols presented here to incorporate biotin and fluorophore at the 5′ and 3′ ends, preserving the 3′ end of the 5′ RNA, and vice versa. Alternatively, the central portion can be chemically synthesized with an internal amino-, azido- or sulfhydryl-modification for subsequent conjugation with a fluorophore following ligation via a DNA splint. By contrast, longer RNAs may not be amenable for labeling using the conjugation methods presented. They can, alternatively, be internally labeled by hybridizing a fluorophore or biotin-labeled synthetic oligonucleotide to extended and/or unstructured regions of the RNA (Fig. 4b). To obtain high melting temperatures between the oligonucleotide and RNA, locked nucleic acids (LNAs) may be used. Although this method does not result in covalent modification of the RNA with the fluorophore or biotin, a high melting temperature of the hybridizing oligonucleotide ensures that the interaction will be sufficiently stable under most experimental temperatures.

It is envisioned that the methods presented in this article will be increasingly used to study RNA dynamics, kinetics of RNA–RNA or RNA–protein interactions particularly for heterogeneously folding RNA to better understand the molecular mechanisms of noncoding RNA function in vivo.

4 Notes

1. The plasmid encoding for the *glmS* ribozyme and binding sequence complementary to the capture strand is available from our laboratory upon request. In order to obtain sufficient plasmid for the transcription reaction, it needs to be transformed into competent cells, such as BL21(DE3) (New England Biolabs), plated onto antibiotic-containing LB-agar plates, cultured, and purified from the cell lysate using a plasmid maxi kit (Qiagen or other supplier).
2. NTPs are stored at −20 °C, and should be freeze–thawed as infrequently as possible. For long-term use, store at −80 °C.
3. Plasmids encoding for the T7 RNA polymerase gene for protein overexpression and purification are available [85] or the enzyme is available for purchase through New England Biolabs.
4. TBE is difficult to dissolve. To overcome low solubility, prepare a 5× stock by mixing 53.9 g of Tris base, 27.5 g boric acid and 3.73 g Na_2EDTA in 800 mL of distilled water. Stir until dissolved, then bring volume up to 1 L.
5. 70 % (v/v) EtOH is made by mixing 35 mL of non-denatured EtOH with 15 mL of double-deionized water.
6. Fluorophores are shipped in light-protective packaging. However, once opened, they should be protected from light by wrapping in aluminum foil to avoid photobleaching.
7. Although yeast PAP can add all four NTPs to the 3′ end of RNA, ATP is the preferred substrate followed by GTP, UTP, and CTP [86]. For better labeling efficiency and to achieve addition of a single 2′-N_3-2′-dNTP, reaction conditions should be first optimized for each NTP. To add a single 2′-N_3-2′-dATP, *E. coli* PAP should be used instead of yeast PAP. Alternatively, 3′-N_3-2′,3′-ddNTPs can be used to add a single base at the 3′ end of RNA; however, it should be noted that if this option is used, RNA ligation can no longer be performed due to the lack of a 3′ hydroxyl group.
8. Oligonucleotides can be synthesized in house, or ordered from companies such as Dharmacon or IDT. Oligonucleotides should be prepared with a 5′ or 3′ primary amine modification for subsequent conjugation to fluorophore dyes through an NHS-ester linkage.

9. Hybridization buffer is used for the hybridization of the fluorophore-labeled oligonucleotide to the RNA of interest. The exact composition of this buffer needs to be optimized for the system on a case-by-case basis. The pH, concentration of monovalent ions and Mg^{2+} ions should be kept near physiological conditions to maintain the co-transcriptional secondary and tertiary fold of the RNA. Alternatively, hybridization of oligonucleotides to unstructured, extended loops on 16S rRNA within the *E. coli* 30S ribosomal subunit requires the use of a Tris-polymix buffer: 50 mM Tris-OAc (pH 7.5), 100 mM KCl, 5 mM NH_4OAc, 0.5 mM $Ca(OAc)_2$, 15 mM $Mg(OAc)_2$, 6 mM β-mercaptoethanol, 5 mM putrescine, and 1 mM spermidine. For RNAs other than 16S RNAs, simpler Tris-buffers can be used.
10. The DNA splint should be the reverse complement of the 5′ end of the downstream RNA strand and the 3′ end of the upstream RNA strand, such that it joins the 3′ hydroxyl of the upstream (or 5′) strand in close proximity of the 5′ phosphate of the downstream (or 3′) strand. Complementarity should extend ~25–30 nt into each RNA strand to ensure a high enough melting temperature and specificity to the RNAs of interest.
11. Slides should be drilled using diamond drill bits (1.0 mm diameter, Kingsley North, Norway, MI) in a high-speed hand drill (Dremel 300-N, Racine, WI) held by a work-station (Dremel 220-01, Racine, WI).
12. 1 M KOH should be prepared fresh about once every month to avoid precipitation of impurities.
13. bBSA can be dissolved to a stock of 1 mg/mL with double-deionized water and stored in separate aliquots.
14. Dissolve dry streptavidin stock in double-deionized water to a concentration of 0.2 mg/mL.
15. Prepare fresh by dissolving 84 mg of sodium bicarbonate in 10 mL double-deionized water.
16. OSS buffer should be prepared fresh immediately before each use. PCA, PCD, and Trolox should each be stored at –20 °C in small aliquots to limit the amount of freeze–thaw cycles each is submitted to.
17. Reaction volume can be scaled up or down depending on the RNA yield desired.
18. Amount of capture strand in the transcription reaction should be optimized as too much will compete for the streptavidin beads, while too little will not be sufficient to bind transcribed RNA efficiently.
19. Place tubes in the MPC and allow beads to attach to the wall of the centrifuge tube. The beads will stick to the walls of the

tube, allowing the supernatant to be drawn out of the tube without disturbing the beads. DynaMag-2 (Invitrogen) is suitable for volumes up to 2 mL, however, other models are available for volumes up to 50 mL.

20. The amount of GlcN6P to affect cleavage needs to be optimized for each system. The values given in the protocols above were optimized for purification of the VS ribozyme, and may vary on a case-by-case basis.
21. Reaction volume can scaled up or down depending on the yield desired.
22. Solid EDC is hygroscopic and should be sealed to be protected from moisture. Weighing should be done quickly.
23. EDC is labile in aqueous solution, therefore, addition of hydrazide derivatives or ethylenediamine and imidazole to the EDC/RNA solution should be done as quickly as possible.
24. Although complete dissolution of biotin hydrazide is essential for the reaction, it will not dissolve completely immediately. The long reaction time ensures that all reactant will dissolve well before the completion of the reaction.
25. NAP-5 columns come pre-equilibrated with a storage buffer. This buffer should be drained before use, and buffer exchanged with ~15 mL of water or TE buffer. Following equilibration, apply the sample to the column bed and allow to enter the column. Elute sample with water or TE buffer. The fraction in which the RNA elutes can be determined by observing the A260 of each fraction.
26. Upon labeling with NHS-ester derivatives, DMSO should compose ≥50 % of the reaction volume to achieve optimal labeling efficiency.
27. RNA can be resuspended in double-deionized water if further labeling steps are to be carried out. However, if the labeling reactions are complete, RNA can be resuspended in a near-physiological buffer for smFRET measurements, such as 50 mM Tris–HCl, pH 7.5, 100 mM KCl, 1 mM $MgCl_2$.
28. Excess unhybridized oligonucleotide does not need to be removed from the RNA/oligonucleotide mix. By binding the RNA to slide via its biotin attachment, all unhybridized oligonucleotide will be washed away.
29. This protocol is for a 20 μl reaction; scale up accordingly for larger volumes. The amounts of RNA oligonucleotides, DNA splint, Rnl-2 enzyme, and reaction time may need to be optimized for better yields on less precious unmodified RNA samples.
30. Proper cleaning of the slides and coverslips is very important to ensure that the slides are free of fluorescent impurities. Wear protective lab coat and goggles while making the slides.

31. Scrubbing of slides is done using gloved hands.
32. If opting to let the slides cool by air, place a sheet of aluminum foil over the slides to shield them from dust in the air.
33. The width of the microfluidic channel should be about 1–2 cm. Upon construction of the channel using pipet tips and capillary tubes, all the weak joints should be sealed with epoxy resin taking care not to get any of it inside the tubes or inside the channel.
34. Proper molecule density should be ~300–400 molecules per field of view. Too few molecules will result in insufficient amount of data, while too many molecules will not allow for the analysis of single molecules because of their spatial overlap.
35. If photobleaching of fluorophores happens too quickly, the concentrations of PCA and PCD can be increased to extend their lifetimes.

Acknowledgments

Work in the authors' laboratory was supported by the NIH grants RO1 GM062357, GM098023, and GM06316.

References

1. Amaral PP, Dinger ME, Mercer TR, Mattick JS (2008) The eukaryotic genome as an RNA machine. Science 319:1787–1789
2. Roth A, Breaker RR (2009) The structural and functional diversity of metabolite-binding riboswitches. Annu Rev Biochem 78:305–334
3. Brodersen P, Voinnet O (2009) Revisiting the principles of microRNA target recognition and mode of action. Nat Rev Mol Cell Biol 10:141–148
4. Wahl MC, Will CL, Luhrmann R (2009) The spliceosome: design principles of a dynamic RNP machine. Cell 136:701–718
5. Steitz TA, Moore PB (2003) RNA, the first macromolecular catalyst: the ribosome is a ribozyme. Trends Biochem Sci 28:411–418
6. Collins K (2006) The biogenesis and regulation of telomerase holoenzymes. Nat Rev Mol Cell Biol 7:484–494
7. Al-Hashimi HM, Walter NG (2008) RNA dynamics: it is about time. Curr Opin Struct Biol 18:321–329
8. Deigan KE, Ferre-D'Amare AR (2011) Riboswitches: discovery of drugs that target bacterial gene-regulatory RNAs. Acc Chem Res 44:1329–1338
9. Serganov A, Huang L, Patel DJ (2008) Structural insights into amino acid binding and gene control by a lysine riboswitch. Nature 455:1263–1267
10. Stoddard CD, Montange RK, Hennelly SP, Rambo RP, Sanbonmatsu KY, Batey RT (2010) Free state conformational sampling of the SAM-I riboswitch aptamer domain. Structure 18:787–797
11. Vicens Q, Mondragon E, Batey RT (2011) Molecular sensing by the aptamer domain of the FMN riboswitch: a general model for ligand binding by conformational selection. Nucleic Acids Res 39:8586–8598
12. Haller A, Rieder U, Aigner M, Blanchard SC, Micura R (2011) Conformational capture of the SAM-II riboswitch. Nat Chem Biol 7:393–400
13. Jenkins JL, Krucinska J, McCarty RM, Bandarian V, Wedekind JE (2011) Comparison of a preQ1 riboswitch aptamer in metabolite-bound and free states with implications for gene regulation. J Biol Chem 286:24626–24637
14. Santner T, Rieder U, Kreutz C, Micura R (2012) Pseudoknot Preorganization of the PreQ(1) Class I Riboswitch. J Am Chem Soc 134:11928–11931

15. Milligan JF, Groebe DR, Witherell GW, Uhlenbeck OC (1987) Oligoribonucleotide synthesis using T7 RNA polymerase and synthetic DNA templates. Nucleic Acids Res 15: 8783–8798
16. Wong TN, Sosnick TR, Pan T (2007) Folding of noncoding RNAs during transcription facilitated by pausing-induced nonnative structures. Proc Natl Acad Sci U S A 104:17995–18000
17. Bhaskaran H, Russell R (2007) Kinetic redistribution of native and misfolded RNAs by a DEAD-box chaperone. Nature 449:1014–1018
18. Russell R (2008) RNA misfolding and the action of chaperones. Front Biosci 13:1–20
19. Uhlenbeck OC (1995) Keeping RNA happy. RNA 1:4–6
20. Pereira MJ, Behera V, Walter NG (2010) Nondenaturing purification of co-transcriptionally folded RNA avoids common folding heterogeneity. PLoS One 5:e12953
21. Marek MS, Johnson-Buck A, Walter NG (2011) The shape-shifting quasispecies of RNA: one sequence, many functional folds. Phys Chem Chem Phys 13:11524–11537
22. Roy R, Hohng S, Ha T (2008) A practical guide to single-molecule FRET. Nat Methods 5:507–516
23. Walter NG, Huang CY, Manzo AJ, Sobhy MA (2008) Do-it-yourself guide: how to use the modern single-molecule toolkit. Nat Methods 5:475–489
24. Pljevaljcic G, Robertson-Anderson R, van der Schans E, Millar D (2012) Analysis of RNA folding and ribonucleoprotein assembly by single-molecule fluorescence spectroscopy. Methods Mol Biol 875:271–295
25. Ditzler MA, Rueda D, Mo J, Hakansson K, Walter NG (2008) A rugged free energy landscape separates multiple functional RNA folds throughout denaturation. Nucleic Acids Res 36:7088–7099
26. Steiner M, Karunatilaka KS, Sigel RK, Rueda D (2008) Single-molecule studies of group II intron ribozymes. Proc Natl Acad Sci U S A 105:13853–13858
27. Bokinsky G, Rueda D, Misra VK, Rhodes MM, Gordus A, Babcock HP, Walter NG, Zhuang X (2003) Single-molecule transition-state analysis of RNA folding. Proc Natl Acad Sci U S A 100:9302–9307
28. Liu S, Bokinsky G, Walter NG, Zhuang X (2007) Dissecting the multistep reaction pathway of an RNA enzyme by single-molecule kinetic "fingerprinting". Proc Natl Acad Sci U S A 104:12634–12639
29. Rueda D, Bokinsky G, Rhodes MM, Rust MJ, Zhuang X, Walter NG (2004) Single-molecule enzymology of RNA: essential functional groups impact catalysis from a distance. Proc Natl Acad Sci U S A 101:10066–10071
30. Zhuang X, Kim H, Pereira MJ, Babcock HP, Walter NG, Chu S (2002) Correlating structural dynamics and function in single ribozyme molecules. Science 296:1473–1476
31. Pereira MJ, Nikolova EN, Hiley SL, Jaikaran D, Collins RA, Walter NG (2008) Single VS ribozyme molecules reveal dynamic and hierarchical folding toward catalysis. J Mol Biol 382: 496–509
32. de Silva C, Walter NG (2009) Leakage and slow allostery limit performance of single drug-sensing aptazyme molecules based on the hammerhead ribozyme. RNA 15:76–84
33. McDowell SE, Jun JM, Walter NG (2010) Long-range tertiary interactions in single hammerhead ribozymes bias motional sampling toward catalytically active conformations. RNA 16:2414–2426
34. Lemay JF, Penedo JC, Tremblay R, Lilley DM, Lafontaine DA (2006) Folding of the adenine riboswitch. Chem Biol 13:857–868
35. Tremblay R, Lemay JF, Blouin S, Mulhbacher J, Bonneau E, Legault P, Dupont P, Penedo JC, Lafontaine DA (2011) Constitutive regulatory activity of an evolutionarily excluded riboswitch variant. J Biol Chem 286:27406–27415
36. Wood S, Ferre-D'Amare AR, Rueda D (2012) Allosteric tertiary interactions preorganize the c-di-GMP riboswitch and accelerate ligand binding. ACS Chem Biol 7:920–927
37. Abelson J, Blanco M, Ditzler MA, Fuller F, Aravamudhan P, Wood M, Villa T, Ryan DE, Pleiss JA, Maeder C, Guthrie C, Walter NG (2010) Conformational dynamics of single pre-mRNA molecules during in vitro splicing. Nat Struct Mol Biol 17:504–512
38. Mihalusova M, Wu JY, Zhuang X (2011) Functional importance of telomerase pseudoknot revealed by single-molecule analysis. Proc Natl Acad Sci U S A 108:20339–20344
39. Hengesbach M, Kim NK, Feigon J, Stone MD (2012) Single-molecule FRET reveals the folding dynamics of the human telomerase RNA pseudoknot domain. Angew Chem Int Ed Engl 51:5876–5879
40. Kieft JS, Batey RT (2004) A general method for rapid and nondenaturing purification of RNAs. RNA 10:988–995
41. Batey RT, Kieft JS (2007) Improved native affinity purification of RNA. RNA 13:1384–1389
42. Vicens Q, Gooding AR, Duarte LF, Batey RT (2009) Preparation of group I introns for biochemical studies and crystallization assays by native affinity purification. PLoS One 4:e6740

43. Di Tomasso G, Lampron P, Dagenais P, Omichinski JG, Legault P (2011) The ARiBo tag: a reliable tool for affinity purification of RNAs under native conditions. Nucleic Acids Res 39:e18
44. Cheong HK, Hwang E, Lee C, Choi BS, Cheong C (2004) Rapid preparation of RNA samples for NMR spectroscopy and X-ray crystallography. Nucleic Acids Res 32:e84
45. Luo Y, Eldho NV, Sintim HO, Dayie TK (2011) RNAs synthesized using photocleavable biotinylated nucleotides have dramatically improved catalytic efficiency. Nucleic Acids Res 39:8559–8571
46. Kim I, McKenna SA, Viani Puglisi E, Puglisi JD (2007) Rapid purification of RNAs using fast performance liquid chromatography (FPLC). RNA 13:289–294
47. Easton LE, Shibata Y, Lukavsky PJ (2010) Rapid, nondenaturing RNA purification using weak anion-exchange fast performance liquid chromatography. RNA 16:647–653
48. Paredes E, Evans M, Das SR (2011) RNA labeling, conjugation and ligation. Methods 54:251–259
49. Qin PZ, Pyle AM (1999) Site-specific labeling of RNA with fluorophores and other structural probes. Methods 18:60–70
50. Walter NG (2001) Structural dynamics of catalytic RNA highlighted by fluorescence resonance energy transfer. Methods 25:19–30
51. Walter NG (2003) Probing RNA structural dynamics and function by fluorescence resonance energy transfer (FRET). Curr Protoc Nucleic Acid Chem Chapter 11:Unit 11 10
52. Li N, Yu C, Huang F (2005) Novel cyanine-AMP conjugates for efficient 5' RNA fluorescent labeling by one-step transcription and replacement of [gamma-32P]ATP in RNA structural investigation. Nucleic Acids Res 33:e37
53. Shu D, Zhang H, Jin J, Guo P (2007) Counting of six pRNAs of phi29 DNA-packaging motor with customized single-molecule dual-view system. EMBO J 26:527–537
54. Paredes E, Das SR (2011) Click chemistry for rapid labeling and ligation of RNA. Chembiochem 12:125–131
55. Richardson RW, Gumport RI (1983) Biotin and fluorescent labeling of RNA using T4 RNA ligase. Nucleic Acids Res 11:6167–6184
56. Winz ML, Samanta A, Benzinger D, Jaschke A (2012) Site-specific terminal and internal labeling of RNA by poly(A) polymerase tailing and copper-catalyzed or copper-free strain-promoted click chemistry. Nucleic Acids Res 40:e78
57. Paredes E, Das SR (2012) Optimization of acetonitrile co-solvent and copper stoichiometry for pseudo-ligandless click chemistry with nucleic acids. Bioorg Med Chem Lett 22:5313–5316
58. Marshall RA, Dorywalska M, Puglisi JD (2008) Irreversible chemical steps control intersubunit dynamics during translation. Proc Natl Acad Sci U S A 105:15364–15369
59. Smith GJ, Sosnick TR, Scherer NF, Pan T (2005) Efficient fluorescence labeling of a large RNA through oligonucleotide hybridization. RNA 11:234–239
60. Solomatin S, Herschlag D (2009) Methods of site-specific labeling of RNA with fluorescent dyes. Methods Enzymol 469:47–68
61. Greenfeld M, Solomatin SV, Herschlag D (2011) Removal of covalent heterogeneity reveals simple folding behavior for P4-P6 RNA. J Biol Chem 286:19872–19879
62. Nichols NM, Tabor S, McReynolds LA (2008) RNA ligases. Curr Protoc Mol Biol Chapter 3:Unit 3 15
63. Zuker M (2003) Mfold web server for nucleic acid folding and hybridization prediction. Nucleic Acids Res 31:3406–3415
64. Joo C, Balci H, Ishitsuka Y, Buranachai C, Ha T (2008) Advances in single-molecule fluorescence methods for molecular biology. Annu Rev Biochem 77:51–76
65. Axelrod D (2003) Total internal reflection fluorescence microscopy in cell biology. Methods Enzymol 361:1–33
66. Haustein E, Schwille P (2007) Fluorescence correlation spectroscopy: novel variations of an established technique. Annu Rev Biophys Biomol Struct 36:151–169
67. Churchman LS, Okten Z, Rock RS, Dawson JF, Spudich JA (2005) Single molecule high-resolution colocalization of Cy3 and Cy5 attached to macromolecules measures intramolecular distances through time. Proc Natl Acad Sci U S A 102:1419–1423
68. Sharonov A, Hochstrasser RM (2006) Wide-field subdiffraction imaging by accumulated binding of diffusing probes. Proc Natl Acad Sci U S A 103:18911–18916
69. Manley S, Gillette JM, Patterson GH, Shroff H, Hess HF, Betzig E, Lippincott-Schwartz J (2008) High-density mapping of single-molecule trajectories with photoactivated localization microscopy. Nat Methods 5:155–157
70. Lund K, Manzo AJ, Dabby N, Michelotti N, Johnson-Buck A, Nangreave J, Taylor S, Pei R, Stojanovic MN, Walter NG, Winfree E, Yan H (2010) Molecular robots guided by prescriptive landscapes. Nature 465:206–210
71. Charvin G, Strick TR, Bensimon D, Croquette V (2005) Tracking topoisomerase activity at

the single-molecule level. Annu Rev Biophys Biomol Struct 34:201–219

72. Ashkin A (1970) Acceleration and Trapping of Particles by Radiation Pressure. Phys Rev Lett 24:156–159
73. Binnig G, Rohrer H, Gerber C, Weibel E (1982) Surface Studies by Scanning Tunneling Microscopy. Phys Rev Lett 49:57–61
74. Schuler B, Eaton WA (2008) Protein folding studied by single-molecule FRET. Curr Opin Struct Biol 18:16–26
75. Bokinsky G, Zhuang X (2005) Single-molecule RNA folding. Acc Chem Res 38:566–573
76. Aleman EA, Lamichhane R, Rueda D (2008) Exploring RNA folding one molecule at a time. Curr Opin Chem Biol 12:647–654
77. Aitken CE, Marshall RA, Puglisi JD (2008) An oxygen scavenging system for improvement of dye stability in single-molecule fluorescence experiments. Biophys J 94:1826–1835
78. Rasnik I, McKinney SA, Ha T (2006) Nonblinking and long-lasting single-molecule fluorescence imaging. Nat Methods 3:891–893
79. Blanco M, Walter NG (2010) Analysis of complex single-molecule FRET time trajectories. Methods Enzymol 472:153–178
80. McKinney SA, Joo C, Ha T (2006) Analysis of single-molecule FRET trajectories using hidden Markov modeling. Biophys J 91: 1941–1951
81. Bronson JE, Fei J, Hofman JM, Gonzalez RL Jr, Wiggins CH (2009) Learning rates and states from biophysical time series: a Bayesian approach to model selection and single-molecule FRET data. Biophys J 97:3196–3205
82. Qin F, Li L (2004) Model-based fitting of single-channel dwell-time distributions. Biophys J 87:1657–1671
83. Spitale RC, Torelli AT, Krucinska J, Bandarian V, Wedekind JE (2009) The structural basis for recognition of the PreQ0 metabolite by an unusually small riboswitch aptamer domain. J Biol Chem 284:11012–11016
84. Suddala KC, Rinaldi AJ, Feng J, Mustoe AM, Eichhorn CD, Al-Hashimi HM, Brooks CL, Walter NG (2013) Single transcriptional and translational riboswitches adopt similar pre-folded ensembles that follow distinct folding pathways into the same ligand-bound structure. Nucleic Acids Res 41:10462–10475
85. He B, Rong M, Lyakhov D, Gartenstein H, Diaz G, Castagna R, McAllister WT, Durbin RK (1997) Rapid mutagenesis and purification of phage RNA polymerases. Protein Expr Purif 9:142–151
86. Martin G, Keller W (1998) Tailing and 3'-end labeling of RNA with yeast poly(A) polymerase and various nucleotides. RNA 4:226–230